The catalytic efficiency of Ru/Mn/Ce-Al_2O_3 in the reduction of HCN in dry methane reforming with CO_2 assisted by non-thermal plasma

David Hong Kian Kok[1], **Raja Kamarulzaman Raja Ibrahim**[2,3], **Susilawati Toemen**[4], **Mohd Bakri Bakar**[4]

[1]Faculty of Electrical Engineering, Universiti Teknologi Malaysia, UTM Johor Bahru,81310 Johor,Malaysia.
[2]Department of Physics, Faculty of Science, Universiti Teknologi Malaysia, 81310, UTMJB, Johor, Malaysia.
[3]Laser Centre, Ibnu Sina Institute for Scientific and Industrial Research (ISI-SIR), Universiti Teknologi Malaysia, 81310 UTM Johor Bahru, Johor, Malaysia
[4]Department of Chemistry, Faculty of Science, Universiti Teknologi Malaysia, 81310, UTMJB, Johor, Malaysia.

Email address: rkamarulzaman@utm.my

Abstract: This study investigates the catalytic activity of Ru/Mn/Ce-Al_2O_3 in eliminating HCN via dry reforming CH_4 with CO_2 in the packed-bed dielectric barrier discharge non-thermal plasma (DBD NTP). A packed bed DBD configuration method was carried out in the non-thermal plasma with Ru/Mn/Ce-Al_2O_3 catalyst, whereby $BaTiO_3$ beads was the dielectric medium. The carrier gas for dry methane reforming was N_2, the peak-to-peak voltage was 24 kV and the total flow rate was 100 sccm with a ratio of 5:5:90 (CH_4:CO_2:N_2), respectively. Gaseous products and by-products were analysed by Fourier transform infra-red (FTIR) spectroscopy. Experimental results revealed that Ru/Mn/Ce-Al_2O_3 catalyst could eliminate HCN at approximately 82% and had a low selectivity in decomposing NH_3. Besides, the conversion of CH_4 achieved was approximately 68%.

1. Introduction

The investigation on the utilization of non-thermal plasma (NTP) in producing value added products (syngas) such as hydrogen for clean and alternative energy, and ammonia for fertilizer production from methane and carbon dioxide has been gaining attention in the past few decades [1-3]. The advantages of NTP assisted dry CH_4 reforming include the capacity to operate at room temperature and atmospheric pressure. Thus, dry CH_4 reforming assisted by NTP is a promising candidate to lead in the transition towards a more sustainable production of valuable products [4].

NTP dissociates and ionizes gaseous species to produce radicals, free electron and ions to initiate and promote chemical reaction that required extreme kinetically and thermodynamically condition such as water-gas shift [5-6], CH_4 reforming with CO_2 [7], as well as ammonia production [8-10] at room temperature and atmospheric pressure.

Although being viewed as a promising alternative to the conventional method in the production of valuable products, NTP has a tendency to produce unwanted-by products that is adverse to the environment and human health. For example, the end-product of NTP CH_4 reforming produces NO_x, which is a powerful greenhouse gas. In addition, NTP produces HCN, which threatens human-health due to its carcinogenic in nature.

To remedy the shortcoming of NTP in CH_4 reforming with CO_2, the introduction of catalyst into the plasma reactor is seen as necessary as it lowers the energy requirement to dissociate the C-H bond of CH_4 bond. This will make the process less prone to form unwanted by-products and enhance conversion. The most widely used catalyst for CH_4 reforming is Al_2O_3 supported with different metal loading especially noble metal to improve stability [11-12]. CeO_2 doped into Al_2O_3 can also improve the catalytic activity of the supported metal oxides through redox cycle [13]. This oxygen exchange and mobility between Ce-Ru and Ce-Mn particles in the catalytic system should plays a significant role in reducing the HCN concentration.

In view of this, our study explores the synergistic effect of Ru/Mn/Ce-Al_2O_3 with non-thermal plasma to improve the effectiveness of CH_4 reforming, consequently improving decomposition and minimizing the formation of HCN.

2. Methodology

2.1. Experimental set-up

The experiments were performed with a coaxial quartz tube with inner diameter of 20 mm. It was filled with packed-bed barium titanate ($BaTiO_3$) beads as the dielectric medium (Figure 1). One experiment was done with 6.0 g of Ru/Mn/Ce-Al_2O_3 beads and another was done without it. The AC voltage ($V_{pk\text{-}pk}$ = 24 kV, f = 22 kHz) was applied between two stainless-steel electrodes with a separation distance of 24 mm. The operational voltage and current were monitored with a high voltage probe (HVP-15HF(TES TEC)) with 1:1000 voltage gain and a high current probe (Fluke80i-400). The electrical signals were analyzed with a PC-based oscilloscope (Picoscope 2208 series). The carrier gas used for the non-thermal plasma reactor was N_2. Both flow rate of CH_4 and CO_2 were set at 5 ml min^{-1} and N_2 was set at 90 ml min^{-1}.

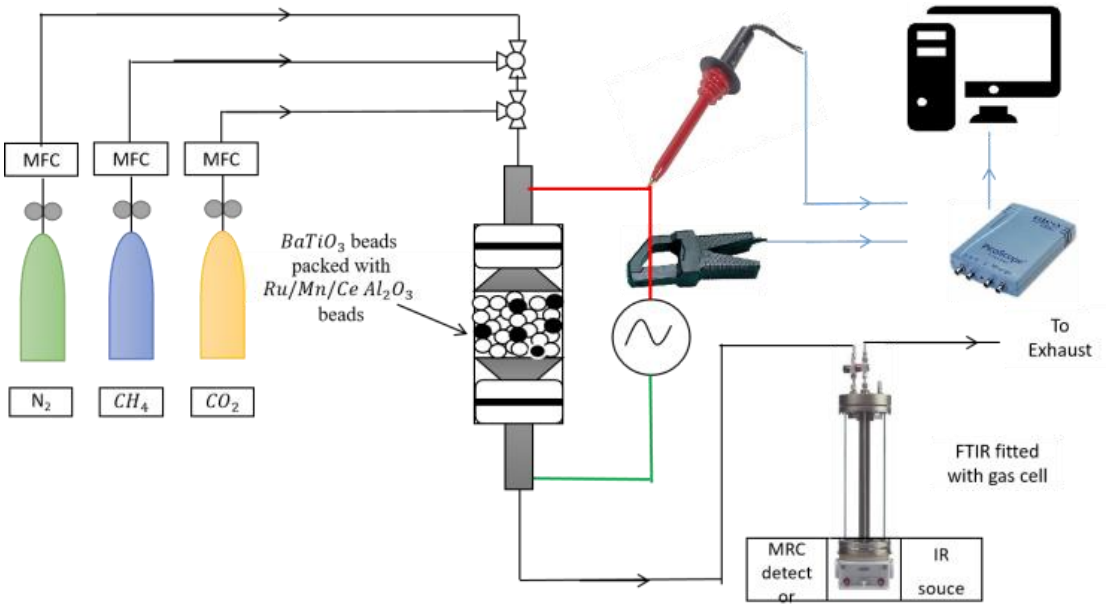

Figure 1. Schematic diagram of DBD non-thermal plasma of methane reforming with CO_2 in the presence of Ru/Mn/Ce-Al_2O_3 catalyst.

The products and by-products of the plasma reactor was fed into a gas cell of optical path length of 8 m (Cyclone C16, Specac). Then, the gas species were analyzed using FTIR (Perkin Elmer, FTIR, NIR, Frontier) with set wavelength of 500 – 4000 cm^{-1}. The scanning rate of FTIR was set at 2 minute per spectrum.

2.2. Method of analysis

Each of the gas species were identified and quantified to obtain its respective concentration. However, not all gas species can be properly quantified due to saturation and overlapping of spectra which are CO_2 and N_2O species. Thus, these species were not investigated. A commercial library provided by Perkin-Elmer inc was used as reference. Each gas species in Figure 2 is set as 100 ppm as concentration, 25 ^oC and at 1 atm.

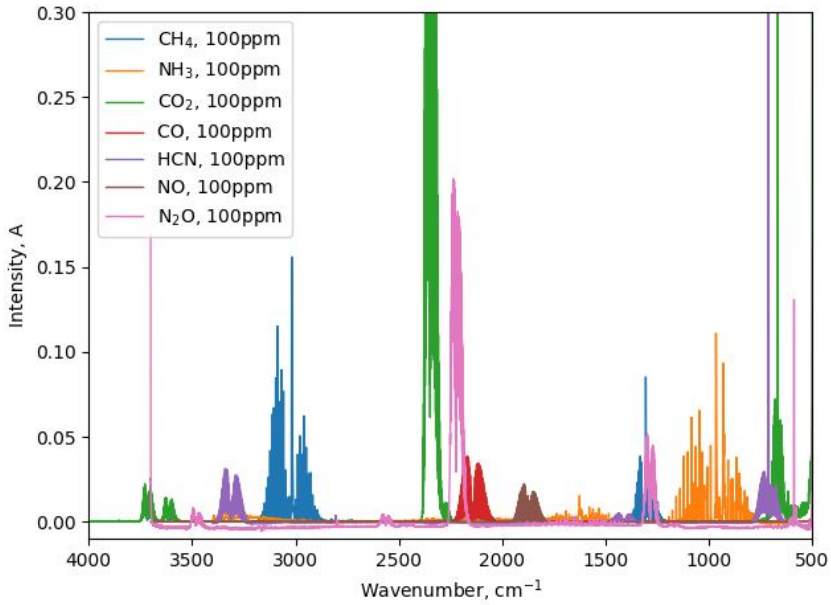

Figure 2. The referred gas species of the products and by-products provided by a commercial library

(1) is the formula used to obtain the concentration of gas species. (2) is used to obtain the percentage conversion of CH_4 and (3) is used to obtain the percentage elimination of HCN.

$$concentration\ of\ gas\ species = \frac{A_{(exp)} N_s L_s}{A_{(ref)} L_m} \tag{1}$$

where,
A(exp) = Area of sample
A(ref) = Area of sample reference at 100 ppm
N_s = concentration of sample reference = 100 ppm
L_s = 1 m
L_m = optical pathlength of gas cell = 8 m

$$\eta_{CH_4}(\%) = \frac{[CH_4(inlet) - CH_4(outlet)](ppm)}{CH_4(inlet)(ppm)} \times 100\,\% \tag{2}$$

$$\chi_{HCN}(\%) = \frac{[HCN\,(without\ catalyst) - HCN\,(with\ catalyst)]}{[HCN\,(without\ catalyst)]} \times 100\,\% \tag{3}$$

3. Discussion

3.1. Influence of Ru/Mn/Ce-Al_2O_3 on the plasma catalytic reaction

Based on Figure 3, at the integration boundary of 3033 – 3200 cm^{-1}, a region where CH_4 exhibits vibrational stretching with peak wavenumber of 3300 cm^{-1} clearly shows that Ru/Mn/Ce-Al_2O_3 accelerated the decomposition of CH_4 with percentage conversion of 68% as compared to 38 % without impregnated the catalyst in the plasma-reactor. The low percentage conversion of CH_4 is attributed to the low temperature

(room temperature) involved in the plasma reaction. Xiaozhong C. *et al* suggested that room temperature hinders the bond activation of C-H bond. The production of activated species such as energetic electrons, nitrogen radicals and UV did not play a significant role in the decomposition of CH_4. It is because the life-time vibrational modes of CH_4 is significantly longer than its excitation and ionization [14], thus more heat are wasted leads to high inefficiency.

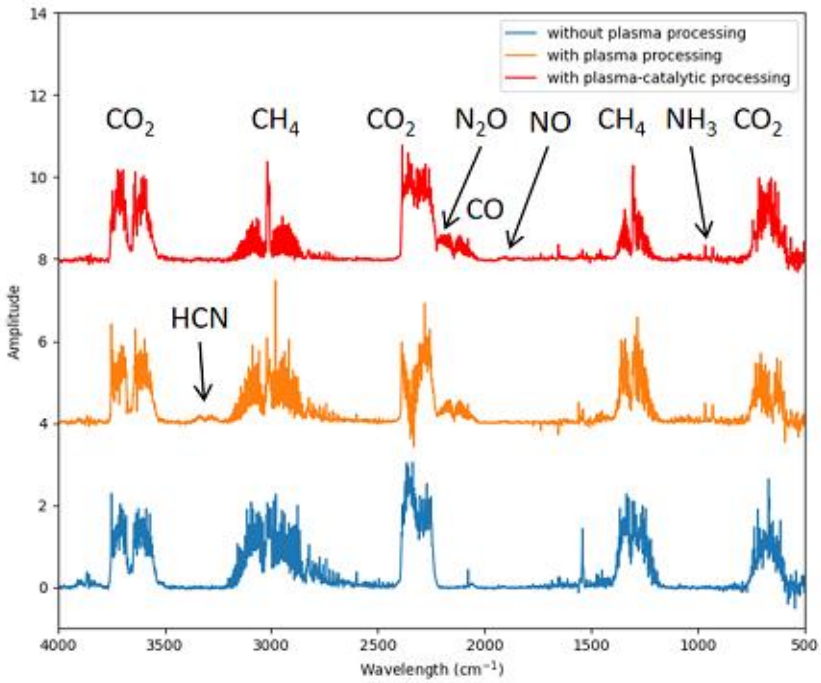

Figure 3. FTIR spectra obtained before and after 10 min (with and without Ru/Mn/Ce-Al_2O_3) plasma processing.

The integration boundary of 3360-3250 cm^{-1} is a region where HCN exhibits vibrational stretching. Figure 3 shows that the presence of Ru/Mn/Ce-Al_2O_3 caused almost complete destruction of the toxic and carcinogenic gas HCN. Whereas without the catalyst, the concentration of HCN is 147 ppm. Nevertheless, HCN is considered an unwanted side-products, thus did not contribute to the significant total volume of valuable products produced in the NTP assisted CH_4 reforming.

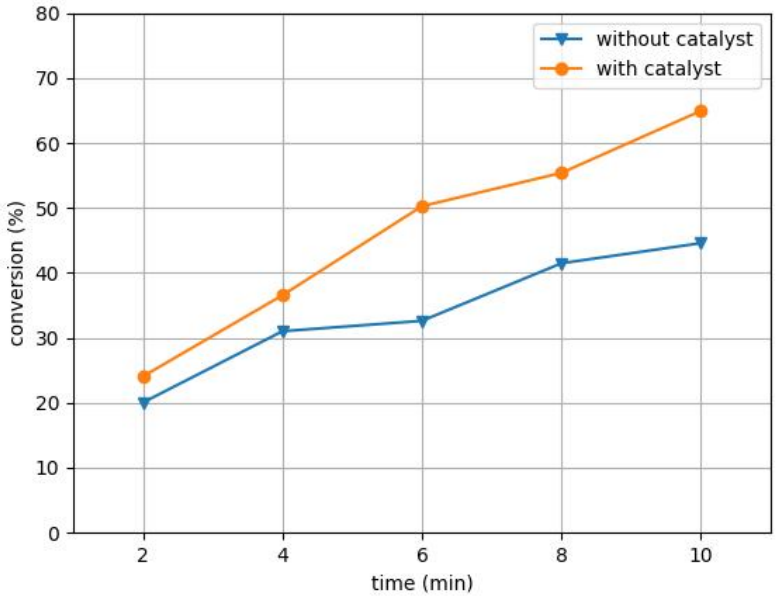

Figure 4. The conversion of CH_4 with and without Ru/Mn/Ce-Al_2O_3 catalyst.

Table 1. The concentration of end products and by-products after treated with NTP.

Gas species	Concentration with catalyst (ppm)	Concentration without catalyst (ppm)
CH_4	642	1178
CO	502	508
HCN	9	148
NH_3	51	89

3.2. Reaction mechanism and chemical Pathway

The enhancement in percentage conversion of CH_4 and the destruction of HCN was the result of redox cycle and oxygen transport of oxides of ruthenium, Ru (RuO_2) and manganese, Mn (MnO_2, Mn_2O_3 and Mn_3O_4). Ru which is considered a noble metal, participates in the decomposition of CH_4. The strong adsorption of CH_4 occurs due to oxygen vacancies created by CeO_2 onto ruthenium oxide. It is suggested that Ce oxides activate Ru oxides and there is an inter reaction between Ru and Ce particles where CeO_2 will exchange oxygen which will promote oxygen vacancies in the Ru metal lattices. This phenomenon will cause oxygen imbalance and activate the catalytic activity by dissociate C-H bond through chemisorption. Besides, chemisorption of CH_4 on the catalyst surface will result in lower of activation energy. Below is the proposed mechanism.

$$CH_4 + Ru \rightarrow CH_3 - Ru + H* \quad (4)$$
$$CH_3* + Ru \rightarrow CH_2 - Ru + H* \quad (5)$$
$$CH_2* + Ru \rightarrow CH - Ru + H* \quad (6)$$

Other than CH_4, Ru metal oxides enhanced the bond activation C=O of CO_2 electronic excitation and ionization [15]. This produced CO ($a^3\pi$) as well as CO_2 ($\chi^2\pi$) state [16]. Although both with and without impregnating Ru/Mn/Ce-Al_2O_3 had no significant influence in the reduction of CO_2 and yields of CO, the oxygen activated species from bond dissociation of C=O was essential as it adsorbed onto the catalyst for oxygen mobility and transportation.

The destruction of HCN are the result of oxygen mobilities and the manifestation of various states of Mn metal valences [22]. It appears that the HCN will likely promote the formation of -CNO species. Below is the proposed mechanism of the decomposition of HCN, where -CNO species will be generated.

$$HCN + MnO_2 \rightarrow H - CNO + Mn_2O_3 \quad (7)$$
$$H - CNO + H_2O \rightarrow NH_3 + CO_2 \quad (8)$$

Ru/Mn/Ce-Al_2O_3 catalyst exhibit basic properties (CeO_2), thus HCN which is acidic easily adsorbed onto the surface of the catalyst. Although -CNO species dominate the proposed mechanism, HCN decomposes without forming -CNO species as intermediary and form -CN species instead [23]. Below is the proposed mechanism (9 - 11).

$$2HCN + 2MnO_2 \rightarrow 2CN* + Mn_2O_3 + H_2O \quad (9)$$
$$CN* + H_2O \rightarrow \bullet NH_2 + CO \quad (10)$$
$$\bullet NH_2 + H* \rightarrow NH_3 \quad (11)$$

Although the formation of HCN is greatly reduced once Ru/Mn/Ce-Al_2O_3 is introduced into the plasma reactor, there is still formation of unwanted side-products such as N_2O and NO (Figure 3). However, formation of NO_2 was not observed. This was due to the conversion of NO with NH_3 selective catalytic reduction (SCR). Similar to the reduction of HCN, reduction of NO also proceed through oxygen transportation and migration of oxygen from Mn metal oxides promoted by Ce particles [24-26]. Below is the proposed mechanism reaction of SCR (12).

$$2NH_3 + 2NO + 2MnO_2 \rightarrow 2N_2 + 3H_2O + Mn_2O_3 \quad (12)$$

The formation of H_2O is essential as a precursor to eliminate HCN as shown in (9). NH_3 is not fully converted in the SCR reaction as it may fully reconverted back in the reduction of HCN.

4. Conclusion

Ru/Mn/Ce-Al_2O_3 successfully eliminate HCN by fully dissociate the carbonated gas species. In turn this enhance the conversion the methane. This is attributed to the combination of unique properties in the catalysis. Redox cycle from Ce particles provides oxygen mobility and transportation in which there is oxygen deficit in the Ru particles. Besides, Ce particles promote the formation of several Mn metal valences to enhance the catalytic activity.

5. Acknowledgement

A special thanks to Universiti Teknologi Malaysia (UTM) for the opportunity to carry out the research and for financial support. This project was supported by Research University Grant - UTM FR (Vot Number:18J84) initiated by UTM.

6. References

[1] Rosha P, Rosha AK, Ibrahim H and Kumar S 2021 A review *Int J Hydrogen Energy* **46** 21318

[2] Zain MM and Mohamed AR 2018 *Renew Sustain Energy Rev* **98** 56-63

[3] Wu J and Zhou XD 2016 *Chinese J Catal* **37** 999

[4] Puliyalil H, Lašič Jurković D, Dasireddy VDBC and Likozar B 2018 *RSC Adv* **8** 27481

[5] Chaudhary R, van Rooij G, Li S, Wang Q, Hensen E and Hessel V 2020 *Chem Eng Sci* **225** 115803

[6] Xu S, Chansai S, Stere C, Inceesungvorn B, Goguet A, Wangkawong, K W, Taylor R, Al-Janabi N, Hardacre C, Martin P A and Xiaolei F 2019 *Nat Catal 2019* **2** 142

[7] Petitpas G, Rollier JD, Darmon A, Gonzalez-Aguilar J, Metkemeijer R and Fulcheri L A 2007 *Int J Hydrogen Energy* **32** 2848

[8] Peng P, Li Y, Cheng Y, Deng S, Chen P and Ruan R. 2016 *Plasma Chem Plasma Process* **36** 1201

[9] Zhou D, Zhou R, Zhou R, Liu B. Zhang T, Xian Y, Cullen P J, Lu X and Ostrikov K. 2021 *Chem Eng J* **421** 129544

[10] Bai M, Zhang Z, Bai X, Bai M and Ning W 2003 *IEEE Trans Plasma Sci* **31** 1285

[11] Lee H, Lee DH, Song YH, Choi WC, Park YK and Kim DH 2015 *Chem Eng J* **259** 761

[12] Kim SS, Kim J, Lee H, Na BK and Song HK. 2005 *Korean J Chem Eng* **22** 585

[13] Vidal H, Kašpar J, Pijolat M, Colon G, Bernal S, Cordon A, Perrichon V and Fally F2000 *Appl Catal B Environ* **27** 49

[14] Mehta P, Barboun P, Go DB, Hicks JC, Schneider WF 2019 *ACS Energy Lett*

[15] Ferreira-Aparicio P, Márquez-Alvarez C, Rodríguez-Ramos I, Schuurman Y, Guerrero-Ruiz A and Mirodatos C. A 1999 *J Catal* **184** 202

[16] Liu Z, Zhang F, Rui N, Li X, Lin L, Betancourt L.E, Su D, Xu W, Cen J, Attenkofer K, Idriss H, Rodriguez J.A and Senanayake S.D, 2019 *ACS Catal* **9** 3349

[17] Sun J, Yamaguchi D, Tang L, Periasamy S, Ma H, Hart J.N and Chiang K 2022 *Adv Powder Technol* **33** 103407

[18] He L, Ren Y, Fu Y, Yue B, Edman Tsang SC and He H 2019 *Mol* **24** 526

[19] Nozaki T and Okazaki K 2013 *Catal Today* **211** 29

[20] Kwak J H, Kovarik L and Szanyi J 2013 *ACS Catal* **3** 2449

[21] Xu S, Chansai S, Shao Y, Xu S, Wang Y.C, Haigh S, Mu Y, Jiao Y, Stere C.E, Chen H, Fan X and Hardacre C 2020 *Appl Catal B Environ*. **268** 118752

[22] Wang L, Wang X, Cheng J, Ning P and Lin Y 2018 *Appl Surf Sci*. **439** 213

[23] Wang X, Cheng J, Wang X, Shi Y, Chen F, Jing X, Wang F, Ma Y, Wang L and Ning P 2018 *Chem Eng J* **333** 402

[24] Wang C, Yu F, Zhu M, Tang C, Zhang Ke, Zhao D, Dong L and Dai B 2019 *J Environ Sci* **75** 124

[25] Zhang L, Pierce J, Leung V L, Wang D and Epling W S 2013 *J Phys Chem C* **117** 8282

[26] Wang C, Yu F, Zhu M, Wang X, Dan J, Zhang J, Cao P and Dai B 2018 *Chem Eng J* **346**182